Wetlands Ecol Manage (2025) 33:12
https://doi.org/10.1007/s11273-024-10027-y

ORIGINAL PAPER

Assessing the feasibility of mapping changes of ecosystem functional groups in South African estuaries using Landsat and Sentinel images of 1990, 2014, 2018 and 2020

Heidi van Deventer · Philani Apleni · Janine B. Adams · Taryn Riddin · Emily Whitfield · Anesu Machite · Lara van Niekerk · Akhona Madasa

Received: 26 April 2024 / Accepted: 16 December 2024

Abstract This study evaluates the feasibility of using medium-resolution satellite sensors to monitor changes in the extent of ecosystem functional groups (EFGs) in South African estuaries, for reporting on the 2030 targets of the Global Biodiversity Framework (GBF). Landsat and Sentinel-1 and -2 image collections in Google Earth Engine (GEE) were used to generate output layers for each of the national land cover years—1990, 2014, 2018 and 2020. Image composites of each year's two growth seasons and one dry season, vegetation indices and topographic data were generated. Changes in the extent and accuracies of three estuarine (mangroves, salt marshes and submerged macrophytes) and three freshwater (forested wetlands, freshwater marshes and large macrophytes) EFGs were calculated and compared to a manually mapped through image interpretation, high-confidence layer. Overall, estuarine EFGs comprised between 10 and 18% of the extent of the EFGs, while freshwater EFGs made up 15% of the extent of estuaries. The overall accuracies of detection of EFGs for 1990 were < 64% compared to the > 71% attained for 2014, 2018 and 2020. In comparison to manual delineations of some of these habitats, the outputs generated from these medium-resolution sensors resulted in overestimation of extent for all EFGs; for mangroves by 115% and for salt marshes and submerged macrophytes by 150–230%. Finer spatial resolution images, and time-series mapping would be critical for

Supplementary Information The online version contains supplementary material available at https://doi.org/10.1007/s11273-024-10027-y.

H. van Deventer (✉)
Council for Scientific and Industrial Research (CSIR), PO Box 395, Pretoria 0001, South Africa
e-mail: HvDeventer@csir.co.za

H. van Deventer · P. Apleni
Department of Geography, Geoinformatics and Meteorology, University of Pretoria, Hatfield, Private Bag X20, Pretoria 0028, South Africa

J. B. Adams · T. Riddin · E. Whitfield · A. Machite · L. van Niekerk
Research Chair in Shallow Water Ecosystems, Department of Science and Innovation–National Research Foundation (DSI-NRF), Department of Botany, Nelson Mandela University, Gqeberha, South Africa

J. B. Adams · T. Riddin · E. Whitfield · A. Machite · L. van Niekerk
Institute for Coastal and Marine Research, Nelson Mandela University, Gqeberha, South Africa

L. van Niekerk
Council for Scientific and Industrial Research (CSIR), Stellenbosch 7600, South Africa

A. Madasa
South African National Biodiversity Institute, Pretoria, South Africa

Published online: 09 January 2025

improved delineation and monitoring of South Africa's estuarine habitats.

Keywords Blue carbon ecosystems · Estuarine habitats · Mangroves · Salt marshes · Seagrasses · Submerged macrophytes

Introduction

Detecting changes in the extent of estuarine habitats is a requirement for reporting to Target 1 of Goal A (ecosystems) of the GBF by 2030 (CBD 2022). The global ecosystem types (Keith et al. 2022) define several EFG for estuaries, including mangroves (MFT1.2 Intertidal forests and shrubland), salt marshes (MFT1.3 Coastal salt marshes and reedbeds), and seagrasses or other submerged macrophytes (M1.1 Seagrass meadows). Several datasets have generated extents of estuarine EFGs and vegetation, habitat and/or land cover types at a global scale using remote sensing image classification. These include the extent of deltas (Tessler et al. 2015), mangroves (Spalding et al. 2010; Giri et al. 2011; Worthington et al. 2020), seagrasses (Green and Short 2003; Short et al. 2007) and salt marshes (Allen Coral Atlas 2020). Mangrove extent has also been updated for the Global Mangrove Watch, including the years 1996, 2007, 2008, 2009, 2010, 2015, 2016 and 2020 (Bunting et al. 2022). The Global Mangrove Watch datasets provide an overview of changes in the extent of mangroves for parts of the world, and is considered an informative monitoring system by the Global Mangrove Alliance (https://www.mangrovealliance.org/).

Global datasets have not assessed the changes in the extent of salt marshes and submerged macrophytes or the degree of representation or change in the extent of these EFGs in finer scale studies. A visual comparison between the most recent datasets and the habitats mapped for South African estuaries (Adams et al. 2016, 2019), showed that the extent of mangroves varies between the Global Mangrove Watch and South African data; an overrepresentation of the extent of seagrasses in Short et al. (2007) and an under-estimation of more than half of the extent of salt marshes in three global datasets (Mcowen et al. 2017; Allen Coral Atlas 2020; Worthington et al. 2023) (Supplementary Information I).

In South Africa, estuarine EFGs have been mapped for some estuaries by ecologists using manual mapping methods such as photo interpretation, heads-up digitising, and vegetation surveys, with or without field surveys, (Adams et al. 2016, 2019) which has resulted in a total of 267 classes across 17 groups (Supplementary Information II). This approach is less desirable for monitoring over time as it can be time-consuming, slow, and ultimately costly. Countries are faced with the challenge of reconsidering the appropriate collection of automated tools in a monitoring framework for ecosystems.

Remote sensing image classification presents an alternative to manual, heads-up digitising, for a consistent approach in mapping and monitoring estuarine EFGs over time. Several studies have illustrated the separability of habitat types across estuarine and freshwater ecosystems both globally and in South Africa. The sensitivity, accuracy, and cost of images from the sensors across various platforms differ. For example, freely available space-borne sensors of the Landsat series of the United States Geology Survey (USGS) offer 30 m spatial resolution images every two weeks but are prone to cloud cover and may not be able to detect narrow extents of habitats and transformed classes. The Sentinel-1 radar and Sentinel-2 optical images of the European Space Agency are also freely available space-borne sensors, but the spatial resolution of bands can be resampled to a 10-m spatial resolution, and images for South Africa are available approximately every five days. These sensors are often referred to as medium spatial resolution, space-borne sensors (Reuter 2011; SEOS 2024).

Images with higher spatial resolutions < 10 m, referred to as fine-scale resolution images (Lillesand et al. 2015; Satellites in Global Development no date a; Satellite Imaging Corporation no date b, 2005; Ustin and Middleton 2021), include two subtypes: (i) those with bands in the red-edge region, that are ideal for vegetation mapping (e.g., WorldView [WV] and RapidEye sensors); and (ii) those with traditional bands (red, green, blue and near infrared; or R, G, B and NIR, respectively) but none in the red-edge region (e.g., the *Satellite pour l'Observation de la Terre* or SPOT). These high spatial resolution sensors and images are, however, costly to purchase and rarely used for extensive monitoring at a country-wide scale (Ustin and Middleton 2021). The use of these images should be selected for particular estuaries, where habitats or vegetation types are narrow or small in extent, and higher spatial resolution images therefore deemed critical or necessary for mapping.

Remote sensing image classification could potentially provide an ideal tool for time-series analysis, that could offer a more consistent approach to the classification of habitat extent across a variety of scales, compared to manual heads-up digitising by individuals. The tools and metrics offered within several remote sensing software packages, speeds up the identification of geographic areas of change, and the quantification of extent and types of changes compared to manual mapping of these habitats (e.g. Bunting et al. 2022). Yet, at the same time, aerial and orthophotograph interpretation may serve as excellent benchmarks to validate the remote sensing image classification outputs against. However, these data do not always exist and may be costly to generate. Outputs from the remote sensing classification of estuarine EFGs remains to be assessed in their positional accuracy and completeness, to evaluate how they can contribute to monitoring and reporting to both the GBF by 2030 (CBD 2022), or the relevant Sustainable Development Goals (SDGs), compared to manual mapping and analysis in geographical information systems.

EFGs are poorly represented in South Africa's NLC datasets for the 4 years of 1990, 2014, 2018 and 2020 (GTI 2015a, 2015b, 2019, 2021), which are used for reporting to national and global targets. To date, the extent of South African mangroves and salt marshes were mapped from a mosaic of several Landsat images over two years, collated from available images between 1 January 2018 and 31 December 2019, to map the extent of these two EFGs (Bessinger et al. 2022). Subclasses that consider the supratidal, intertidal and subtidal regions of the salt marshes and seagrasses can further divide EFGs to a 4th level of the global ecosystem types (Keith et al. 2022), which would facilitate refined habitat monitoring and reporting. Regional variation of remote sensing image classification accuracies along the coast, ranging from the arid west coast to the subtropical east coast, can also contribute to improved understanding of the suitability of the images for monitoring these regions. This study aimed to expand on this initial work by using optical Landsat 5–8 and Sentinel-2 optical images, as well as the radar Sentinel-1 sensors, for quantifying changes in estuarine EFGs. The objectives were to (a) determine the accuracies of mapping estuarine EFGs of South Africa per subclasses and subregions; (b) quantify the changes in extent of the estuarine EFGs that have occurred in these over four time periods; and (c) evaluate the confidence of changes in these EFGs that was generated from the medium-spatial resolution image classification process.

Materials and methods

Study area

A total of 332 South African estuarine systems (290 estuaries[1] and 42 micro-estuaries) were included in the remote sensing analysis. These systems had been delineated and their boundaries updated during the latest National Biodiversity Assessment of 2018 (Van Niekerk et al. 2019; Van Deventer et al. 2020). The coast was subdivided into four earth observation (EO) classification regions for the classification process, based on historic and current presence of mangroves and submerged macrophytes, to avoid overprediction of these in other estuaries where they do not occur (Fig. 1). For the mangrove EO region, all estuaries between the Nahoon and Kosi estuaries were included, as well as the Tyolomnqa Estuary where mangroves were artificially planted. The region included 32 estuaries with known locations of mangroves (Raw et al. 2023), which had historical extent data for mangroves, and another 164 where fine-scale validation would be required.

The division into the four EO regions showed dominance of estuaries (207 or 62% of the total of 332 estuarine systems) in the mangrove EO region

[1] In South Africa, an estuary is defined as a partially enclosed permanent water body, either continuously or periodically open to the sea that extends as far as the upper limit of tidal action, salinity penetration or back-flooding under closed mouth conditions. During high catchment flows or floods an estuary can become a river mouth with no seawater entering the formerly estuarine area or, when there is little or no fluvial input, an estuary can be isolated from the sea by a sandbar and become fresh or even hypersaline. Micro-estuaries are defined as small, permanent coastal water bodies in which mixing of salt- and freshwater can periodically occur owing to overwash from the sea or tidal exchange following breaching of the mouth. These small systems support low densities of a limited number of estuarine and marine species (Van Niekerk et al. 2019).

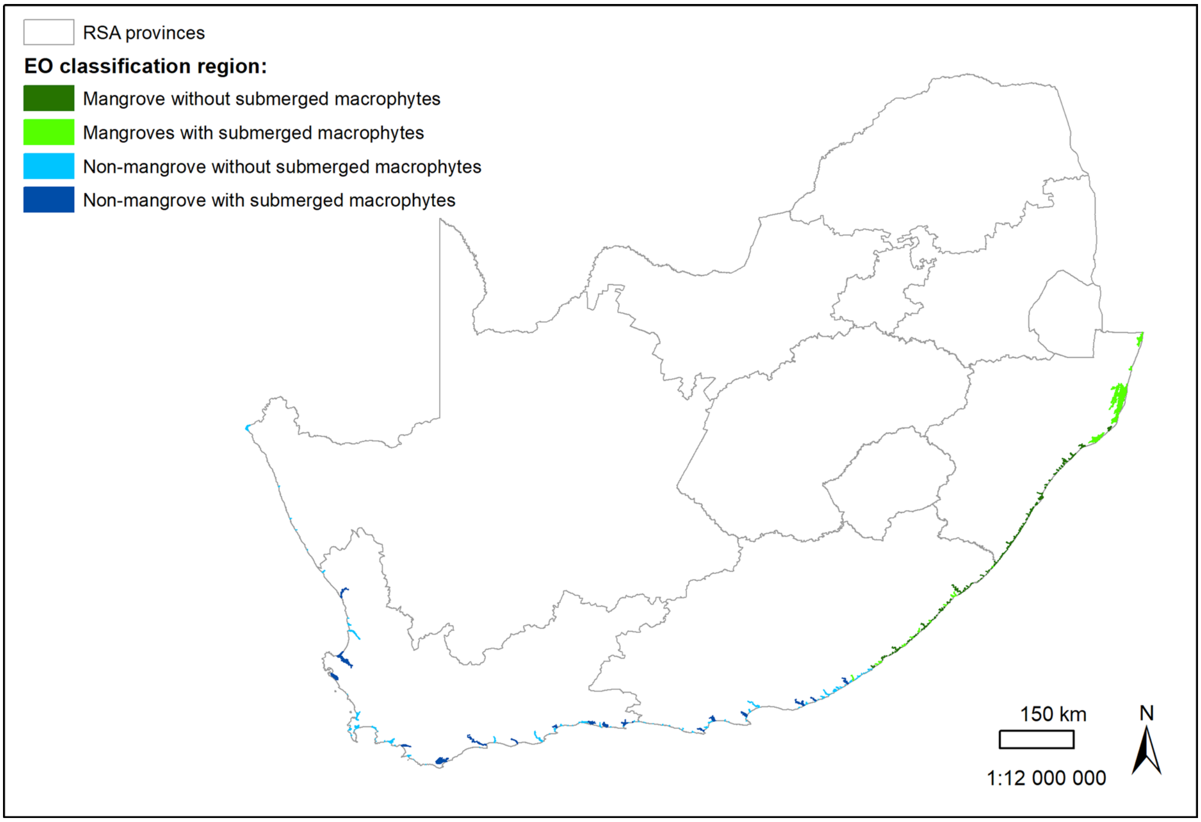

Fig. 1 A total of 290 estuaries and 42 micro-estuaries (total 332 estuarine systems) for South Africa were used in the classification and divided into four subgroups as Earth Observation (EO) classification regions used for the remote sensing classification process

compared to the non-mangrove EO region (38%) (Table 1). Only 12% of the 332 estuarine systems of South Africa are estimated to host submerged macrophytes (which include marine species like the seagrass *Zostera capensis*, as well as brackish species like *Ruppia* spp and *Stuckenia* spp.) Table 1. In both regions, the majority of estuarine systems had no submerged macrophytes recorded in the Nelson Mandela University (NMU) national botanical database layer (Adams et al. 2016, 2019) or as sample points mapped for this project (90% for mangrove and 85% for non-mangrove EO region).

Table 1 Number of estuaries and micro-estuaries per earth observation (EO) remote sensing classification region

	With submerged macrophytes	Without submerged macrophytes	Subtotals
(a) Mangrove EO region: 207 estuaries (62%)			
Estuary	19 (6%)	159 (48%)	178 (54%)
Micro-estuary	1 (< 1%)	28 (8%)	29 (9%)
(b) Non-mangrove EO region: 125 estuaries (38%)			
Estuary	19 (6%)	93 (28%)	112 (38%)
Micro-estuary	0 (0%)	13 (4%)	13 (4%)
Subtotals	39 (12%)	293 (88%)	

The percentage (%) of each subregion is calculated out of the total of 332 estuarine systems

Typology of estuarine ecosystem functional groups

The global EFGs that were identified for inland waters (estuarine and freshwater realms) in the International Union of Conservation of Nature's (IUCN's) global ecosystem types (Keith et al. 2022) were used to define the estuarine and freshwater categories. These include mangroves (MFT1.2 Intertidal forests and shrubland), salt marshes (MFT1.3 Coastal saltmarshes and reedbeds), and submerged macrophytes (not listed as an EFG) for the estuarine realm, and forested wetland (Transitional Forest [TF] 1.2 'sub-tropical-temperate forested wetlands') and freshwater marshes (TF1.4 Seasonal flood-plain marshes and TF1.3 Permanent marshes) for the freshwater realm. A third EFG was proposed by Van Deventer et al. (2022) being large macrophytes, that are predominantly associated with freshwater systems occurring within and outside the estuarine systems, and includes *Cyperus papyrus*, *Phragmites australis* or *mauritanus*, and *Typha capensis*. All six of these EFGs may occur within the estuarine boundaries mapped, with freshwater realms fringing the estuarine habitats, and forming an ecotone that may not always be a geographic definitive boundary, but a mixture of species that can be associated with different habitats. Common reed (*Phragmites australis*) is found in over 50% of South African estuaries (Adams et al. 2016, 2019) where they play an important ecological role in the fresh and brackish zones of estuaries (Adams et al. 2016).

Estuarine reference map layer and classes

The South African estuarine habitat classification system and NMU national botanical database layer (Adams et al. 2016, 2019; hereafter 'NMU layer') present manual maps of 267 macrophyte types or ecotones and a range of land use/land cover classes through heads-up digitising from a diverse number of images to track changes in estuarine habitats. These classes were grouped into 17 general classes to be used in the remote sensing classification, of which some classes concur with the IUCN EFG classes, which allow for the capturing of narrower habitat types and transformed land use/land cover classes than what would be feasible when coarser, spatial resolution space-born images are used for the classification. This database was used as a reference layer to which the remote sensing image classification outputs were compared in the Discussion section.

Remote sensing data acquisition, pre-processing, and analysis

The remote sensing classification was undertaken across four processing phases, including (a) sample preparation and validation, (b) generating image composites for each year in GEE, (c) executing the remote sensing image classification in GEE and (d) integrating the data with the transformed land cover categories of the NLC products (Fig. 2). The following four sub-sections detail the steps taken as part of the workflow for generating the spatial outputs for each of the four selected years, 1990, 2014, 2018 and 2020.

Generating regions of interest (ROIs) for remote sensing classification of estuarine ecosystem functional groups

This phase consisted of four subphases as per Fig. 2, with a description of the relevant steps undertaken under each phase explained in Supplementary Information III:

- (a1) Automated extraction of points from the NMU manually-mapped layer
- (a2) Validation of sample points using Google Earth Pro (GEP 1985–2022) images
- (a3) Capturing of additional samples points in Google Earth Pro for selected classes
- (a4) Spatial integration and translation of sample point classes from all datasets to a single file per year with consistent class names

These steps resulted in more than 12,000 points being available for each year for classification, though the numbers varied per class (Table 2).

Use of multi-seasonal images for classification

Previous work has shown that for the tropical and subtropical coastal systems, located within the summer rainfall region of the country, the best time for habitat classification is in the spring and summer (Van Deventer et al. 2017, 2020), when the majority of the plant nutrients are mobilised towards the leaves of evergreen tree species (mangroves and forested wetlands). However, the combination of all four seasons maximised the separability between six evergreen wetland tree species and other classes (Van Deventer et al. 2017, 2020).

While capturing the sample points in the project, it was also observed that the extent of supratidal salt marshes was maximised in the dry season during low tides on the Google Earth Pro images. A decision was therefore made to include the dry, winter season for all rainfall regions which offers the

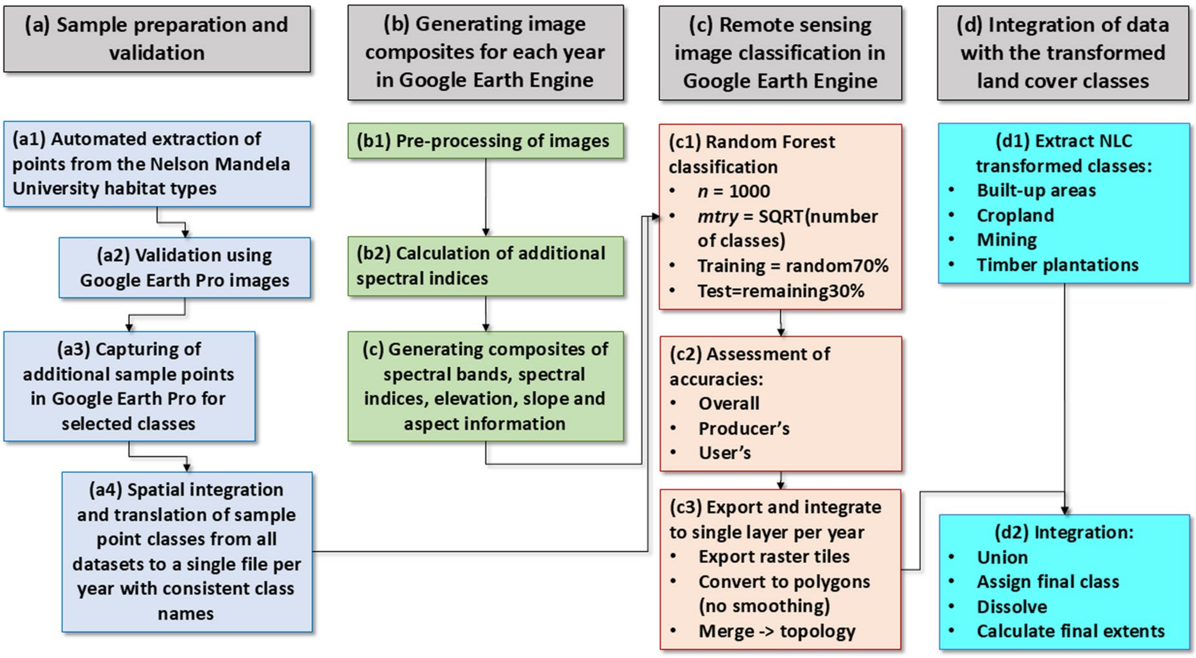

Fig. 2 Workflow showing the overall steps in the remote sensing image classification of the extent of estuarine ecosystems or estuarine Ecosystem Functional Groups (EFGs). The overall phases included (**a**) preparation of sampling points per class; (**b**) generating of image composites; (**c**) execution of the remote sensing image classification and (**d**) accuracy assessment

mapping of salt marsh extent during low inundation regimes. The combination of the growth season with the dry season, across various tidal ranges, will also enhance the separability between some of the supratidal, intertidal and subtidal classes. Therefore, for these EO regions, a 17 month period was selected for each year to be classified, ranging from the 1st of September before the selected NLC year, to the 28th of February after the selected NLC year (Table 3).

Selection and pre-processing of satellite images

GEE (Gorelick et al. 2017) was chosen as the platform to process the outputs, considering the capabilities of this cloud-computing platform in managing extensive areas and number of images, compared to individual desktop machines. The pre-processing of the Landsat series of images, and the Sentinel-1 and -2 datasets, as well as the spectral indices used, are explained in Supplementary Information IV.

Classification of satellite images

The Random Forest (Breiman 2001) classifier was used for the classification of the estuarine EFGs and other classes within the estuaries. Random Forest is a non-parametric algorithm known for managing large datasets with low representation in numbers of samples (Van Deventer et al. 2017; Weitkamp and Karimi 2023). Spectral reflectance data show predominantly a non-normal distribution, and non-parametric classifiers have improved the accuracy of classification of spectral data above traditional classifiers that assume normal distribution. In addition, the Random Forest algorithm has been successfully used in several wetland classification studies (e.g., Mahdianpari et al. 2020; Van Deventer et al. 2022).

In the GEE platform, the Smile Random Forest (ee.Classifier.smileRandomForest) was used for the classification of the estuarine EFGs and other classes. The *ntree* was set at 1000, whereas the *mtry* variable defaults for classification to the square root of the number of classes used. The training data was

Table 2 Number (Nr.) of sample points generated per class used for the remote sensing classification of estuarine ecosystem functional groups (EFGs) in alignment for 4 years (1990, 2014, 2018 and 2020) of the National Land Cover (NLC) products of South Africa (GTI 2015a, 2015b, 2019, 2021). The number of regions of interest (ROIs) used for classification was done across four earth observation (EO) regions, including areas without mangroves, those with mangroves, and those with submerged macrophytes or without

				Non- mangroves EO region				Mangrove EO region				Total			
Class name	Description and dominant species	Related habitat type mapped in the NMU layer	Class integer used in GEE	Nr.1990	Nr.2014	Nr.2018	Nr.2020	Nr.1990	Nr.2014	Nr.2018	Nr.2020	Nr.1990	Nr.2014	Nr.2018	Nr.2020
Bare soil	Bare soils were detected around Verlorenvlei Estuary in 2020 and added, some areas possibly peat	Beach and dune sand	1	0	0	0	49	0	0	0	0	0	0	0	49
Beach sand	Areas on the seaside of the estuarine mouth that are dominated by sand		2	59	53	53	50	81	81	81	81	140	134	134	131
Built-up areas	Built-up areas of the NLCs	Developed	3	184	186	185	186	79	79	79	79	263	265	264	265
Cleared land	Areas where the vegetation had been removed	Disturbed	4	37	8	18	0	0	2	8	3	37	10	26	3
Cropland	All agricultural croplands included in the NLCs	Developed (agriculture)	5	98	106	110	100	141	146	146	146	239	252	256	246
Cultivated wetlands	Wetlands that have been transformed into cropland	N.A	6	0	0	0	0	0	160	211	246	0	160	211	246

Table 2 (continued)

				Non- mangroves EO region				Mangrove EO region				Total			
Class name	Description and dominant species	Related habitat type mapped in the NMU layer	Class integer used in GEE	Nr.1990	Nr.2014	Nr.2018	Nr.2020	Nr.1990	Nr.2014	Nr.2018	Nr.2020	Nr.1990	Nr.2014	Nr.2018	Nr.2020
Forested wetland	13 indicator tree species listed in Van Deventer et al. (2021). 'Forested wetlands' is the official IUCN category that includes floodplain, riverine and swamp forests	Swamp forests	7	0	0	0	0	849	687	635	599	849	687	635	599
Freshwater marsh	Freshwater wetlands dominated by grasses and sedges of < 1.5 m in height	Reeds and sedges	8	0	1	1	2	497	499	499	499	497	500	500	501
Intertidal salt marsh (Other)	Intertidal salt marshes where the dominant species cannot be distinguished	Intertidal salt marsh	9	62	35	35	35	23	23	23	23	85	58	58	58
Intertidal salt marsh (*Spartina maritima*)	Intertidal salt marshes dominated by *Spartina maritima*		10	49	49	49	49	7	7	7	7	56	56	56	56
Intertidal salt marsh (Succulent)	Intertidal salt marshes dominated by succulent vegetation		11	272	272	272	272	13	13	13	13	285	285	285	285

Table 2 (continued)

				Non- mangroves EO region				Mangrove EO region				Total			
Class name	Description and dominant species	Related habitat type mapped in the NMU layer	Class integer used in GEE	Nr.1990	Nr.2014	Nr.2018	Nr.2020	Nr.1990	Nr.2014	Nr.2018	Nr.2020	Nr.1990	Nr.2014	Nr.2018	Nr.2020
Large macrophytes	Freshwater ecosystems that are dominated by large macrophytes > 1.5 m in height, including *Cyperus papyrus*; *Phragmites australis* and/or *P. mauritanus*, and *Typha capensis*	Reeds and sedges	12	327	330	331	331	537	539	534	539	864	869	865	870
Mangroves	Five dominant species are included, being *Avicennia marina*, *Bruguiera gymnorhiza*, *Ceriops tagal*, *Lumnitzera racemosa*, *Rhizophora mucronata*, and *Xylocarpus granatum*	Mangroves	13	0	0	0	0	651	654	654	654	651	654	654	654
Mining	Areas where mining is visible	Developed	14	219	182	195	194	0	0	0	0	219	182	195	194
Nymphaea spp.	Floating *Nymphaea* spp. (water lilies)	Freshwater floating macrophyte	15	0	0	0	0	20	20	20	20	20	20	20	20

Table 2 (continued)

				Non- mangroves EO region				Mangrove EO region				Total			
Class name	Description and dominant species	Related habitat type mapped in the NMU layer	Class integer used in GEE	Nr.1990	Nr.2014	Nr.2018	Nr.2020	Nr.1990	Nr.2014	Nr.2018	Nr.2020	Nr.1990	Nr.2014	Nr.2018	Nr.2020
Open water	Wetlands from the lacustrine biome that are predominantly open water features with no permanent or seasonal plant growth across > 90% of the extent of the waterbody	Open water	16	989	980	977	911	618	617	615	616	1607	1597	1592	1527
Relic gardens	Areas of freshwater or salt marsh where previous subsistence farming/agriculture took place	N.A	17	0	0	0	0	123	123	123	123	123	123	123	123
Sand/mudbanks	Areas that are predominantly situated inland of the estuarine mouth and dominated by a range of sand to mudbank flats. These exclude beach and dune sands	Beach and dune sand	18	215	229	230	252	93	96	95	97	308	325	325	349

Table 2 (continued)

Class name	Description and dominant species	Related habitat type mapped in the NMU layer	Class integer used in GEE	Non- mangroves EO region				Mangrove EO region				Total			
				Nr.1990	Nr.2014	Nr.2018	Nr.2020	Nr.1990	Nr.2014	Nr.2018	Nr.2020	Nr.1990	Nr.2014	Nr.2018	Nr.2020
Submerged macro-phytes (intertidal *Zostera*)	Areas of sub-merged macro-phytes that are intertidal and predominantly *Zostera capensis* (eelgrass)	Submerged macro-phytes	19	476	477	484	484	47	47	47	47	523	524	531	531
Submerged macro-phytes (Other)	Submerged mac-rophyte other than *Zostera capensis*. e.g., *Halodule uni-versis* in Kosi Estuary		20	37	36	32	30	215	215	215	215	252	251	247	245
Submerged macro-phytes (subtidal *Zostera*)	Areas of sub-merged macro-phytes that are subtidal and predominantly *Zostera capensis*		21	469	469	469	469	132	132	132	132	601	601	601	601

Table 2 (continued)

				Non- mangroves EO region				Mangrove EO region				Total			
Class name	Description and dominant species	Related habitat type mapped in the NMU layer	Class integer used in GEE	Nr.1990	Nr.2014	Nr.2018	Nr.2020	Nr.1990	Nr.2014	Nr.2018	Nr.2020	Nr.1990	Nr.2014	Nr.2018	Nr.2020
Supratidal salt marsh (*Juncus*)	Salt marsh dominated by the species *Juncus kraussii*	Supratidal salt marsh	22	47	48	48	48	374	374	374	374	421	422	422	422
Supratidal salt marsh (Other)	Supratidal salt marshes that are dominated by other vegetation (excluding *Juncus kraussii* or saline grasses)		23	775	793	801	807	82	82	82	82	857	875	883	889
Supratidal salt marsh (Saline grasses)	Salt marsh dominated by the saline grasses e.g. *Sporobolus virginicus*		24	10	10	10	10	47	47	47	47	57	57	57	57

Table 2 (continued)

				Non- mangroves EO region				Mangrove EO region				Total			
Class name	Description and dominant species	Related habitat type mapped in the NMU layer	Class integer used in GEE	Nr.1990	Nr.2014	Nr.2018	Nr.2020	Nr.1990	Nr.2014	Nr.2018	Nr.2020	Nr.1990	Nr.2014	Nr.2018	Nr.2020
Terrestrial grasses	Terrestrial grasses < 1.5 m in height	Terrestrial	25	65	48	44	48	326	326	326	326	391	374	370	374
Terrestrial shrubs	Terrestrial vegetation > 1.5 m in height but not considered trees		26	46	91	109	112	15	9	9	9	61	100	118	121
Terrestrial trees/forests	Terrestrial trees and forests with heights > 1.5 m and visible canopy structures		27	103	111	98	110	1980	2215	2217	2217	2083	2326	2315	2327
Terrestrial vegetation	Grouping of all types of terrestrial classes		28	407	404	395	394	54	56	54	54	461	460	449	448
Timber plantations	Commercial and subsistence timber plantations including *Eucalyptus* and Pine species		29	0	0	0	0	523	523	523	523	523	523	523	523
Total				4948	4920	4948	4945	7530	7775	7772	7774	12,478	12,695	12,720	12,719

EO earth observation, *GEE* Google Earth Engine, *NMU* Nelson Mandela University, *IUCN* International Union for Conservation of Nature randomly selected at 70% of the total number of the sample points per class, and the remaining 30% used for the testing. The raster result produced was generated at a 30 m spatial resolution for 1990 and 2014, and 10 m spatial resolution for 2018 and 2020.

For each year and class, the percentage of overall (OA%), producer's (PA%) and user's (UA%) accuracies (Story and Congalton 1986) were computed for reporting in GEE. An error matrix was used to report the spectral overlap between classes to inform the improvements. Classes with user's accuracies > 70% could potentially be considered sufficient for reporting of the extent of the estuarine ecosystem functional groups, however, a visual comparison of the image classification outputs to the manually-mapped layer was also undertaken, and comparisons of the extent of the EFGs predicted in the remote sensing classification of the year 2020, was compared to assess the percentage overlap per grouped class of estuarine EFGs, namely for mangroves, salt marshes and submerged macrophytes.

The raster output layers are generated in GEE as unprojected, Geographic World Geodetic System of 1984 (WGS84) tiles, and were subsequently converted from raster to polygon layers in ArcGIS 10.7 into a geodatabase. The polygons were then merged into a single layer and projected to the Albers Equal Area (AEA) coordinate system of South Africa that is used for all ecosystem extent layers, with 25°E as the central longitudinal meridian, and the two parallels of 24° and 33°S. AEA minimises the distortion of the extent of polygons (Snyder 1987, 1993). The transformed classes of the NLC layers were then masked out for the purpose of reporting the extent of estuarine EFGs only.

Integration of data with the transformed land cover classes

Four transformation classes of the NLC output layers, including built-up areas, croplands, mining and timber plantations, were considered for each NLC class of the 4 years of study. The NLC raster datasets pixels were extracted in ArcGIS 10.7 (Extract by Mask under Spatial Analyst) using the 50 m buffered extent of the estuarine system. The raster outputs were then converted from raster to polygons without any simplification, to obtain the spatially most accurate extent of the original pixels. The transformed land cover classes were then extracted for each year, and unioned with the EFG output polygons. Lastly, the polygon layer was clipped to the original extent of the estuaries (excluding the shoreline part) and the total extent of each class calculated in hectares, using the AEA coordinate system.

Results

Remote sensing classification results

The results of the remote sensing classification showed a general increase in the extent of mangroves and salt marshes between 1990 and 2020, while submerged macrophytes initially appeared to decline from 1990 to 2018, and then increased in 2020 (Fig. 3). The overall accuracies (OA) for the last three years were > 71.2% in all EO classification subregions, whereas the 1990 classifications had an OA of 58–73% (Table 4). These results suggest that overall, the 1990 classification shows poor representability of class accuracies compared to the other three years and should be interpreted with caution.

The user's accuracies of the mangroves were 53% and 66% in the no-submerged and submerged subregions, respectively, for 1990 and ≥ 81% for 2014, 2018 and 2020 (Table 4). Upon closer inspection and comparison of the outputs, it was evident that the Landsat images do not detect all mangrove extents, particularly narrow and fragmented patches. The availability of Landsat 7 and 8 images tripled in number for the 2014 classification, compared to the 30 Landsat 5 images used for 1990, which contributed to the improved accuracies reported for 2014. In comparison, the 10 m spatial resolution Sentinel images visibly improved on the omission errors of Landsat, but showed some commission errors upstream and above the 5 m a.m.s.l. height, that would unlikely be mangrove. The 2020 extent (Fig. 3) was 151% of the extent mapped through heads-up digitising from aerial and Google Earth Pro images in the 7 March 2023 layer compared to the NMU layer, which could be considered an unacceptably high degree of overprediction for reporting.

The remote sensing classification of six salt marsh classes were undertaken across all four EO remote sensing classification regions, with three intertidal (other, *Spartina maritima* and succulent) and three

Table 3 Temporal ranges used for the classification of estuarine ecosystem functional groups in South Africa

Sensors	Landsat			Sentinel	
Periods	L5	L7	L8	S1	S2
1 September 1989–28 February 1991	✓				
1 September 2013–28 February 2015	✓	✓	✓		
1 September 2017–28 February 2019				✓	✓
1 September 2019–28 February 2021				✓	✓

Landsat 5 (L5) was operational 1 March 1984–5 June 2013; Landsat 7 (L7): 15 April 1999–6 April 2022; Landsat 8 (L8): 11 February 2013 to date; Sentinel-1A (S1): 3 April 2014; Sentinel-1B (S1): 25 April 2014; Sentinel-2A (S2): 23 June 2015; Sentinel-2B: 7 March 2017

supratidal (*Juncus kraussii*, saline grasses and other). In the Mangrove EO region, the intertidal salt marsh and *Spartina maritima* attained high user's accuracies > 78% for 2014, 2018 and 2020, although the user's accuracy for *Spartina maritima* was only 67% in 2020 (Table 4). *Juncus kraussii* and other supratidal salt marshes showed variation across the estuaries, and sometimes attained user's accuracies > 70%, but in other years then again between 27 and 68%. An insufficient number of sample points for the class 'Saline grasses supratidal salt marshes' in the mangrove EO region resulted in a single point being either 100% accurately classified for some years, but in other years achieving 43% or 44% user's accuracy. In the non-mangrove region, the intertidal salt marshes show no results to very low user's accuracy (33% in 1990 for non-mangrove and no sub-merged macrophyte region; Table 4). The other classes varied from 38 to 85% (ignoring 100% for single sample points per class). The supratidal salt marshes (other) ranged across both mangrove subregions and all four years between 54 and 67%. In comparison to the 7 March 2023 edition of the estuarine habitats layer, the remote sensing image classification predicted double the amount of salt marshes in 2020 (3 261.4 ha, Fig. 3) compared to 12 153 ha mapped in the NMU manually-mapped layer.

Submerged macrophytes had three subclasses: intertidal *Zostera capensis*, subtidal *Zostera capensis* and other classes (Table 4). Of these, the 'other' class overpredicted for the full extent of the open water class in the mangrove EO regions, while attaining user's accuracies of > 85% for all four years (Table 4).

Changes that could not be predicted

Changes in the extent of natural land cover classes other than the estuarine EFGs were observed in some of the estuaries, such as the iMfolozi/uMsunduze (Fig. 4) and Verlorenvlei (Fig. 6) estuaries. Cloud cover obscured the classification in 1990 for the iMfolozi/uMsunduze Estuary (a part of the wider St Lucia Estuarine Lake Complex), but for the other years, the transformation from forested wetlands to cropland (mainly banana plantations) is evident (Fig. 4a) and was also reported and quantified by other studies (Apleni et al. xxxx; Van Deventer et al. 2021).

Changes in the smaller estuaries with narrowed extents did show representation of the different EFGs, and could be useful for reporting extent changes over time, such as the Mnyameni and Mtolane estuaries, for example (Fig. 5). In these systems the extent of mangroves appears to be expanding over the years, whereas the submerged macrophytes showed higher degrees of changes in extent, location and subtypes. These increases may however be unreliable, considering the overprediction of the extent of these EFGs, and not be a reflection of true expansion over this time period. Drought and over-abstraction of water in the Verlorenvlei Estuary have led to a significant reduction in open water, exposure of peat area and increase in large macrophytes over the four time periods (Fig. 6).

Discussion

This study assessed the feasibility of freely available, space-borne Landsat and Sentinel-1 and -2 images for mapping changes in estuarine EFGs of South Africa. Overall, three classes in estuarine EFGs were mapped, including mangroves, submerged macrophytes and salt marshes, as biodiversity types related to the global ecosystem types (Keith et al. 2022). Although changes in these three EFGs were observed between 1990, 2014, 2018 and 2020, the accuracies are discussed in the following subsection, in relation to comparative studies and findings to assess the feasibility of using these results for reporting.

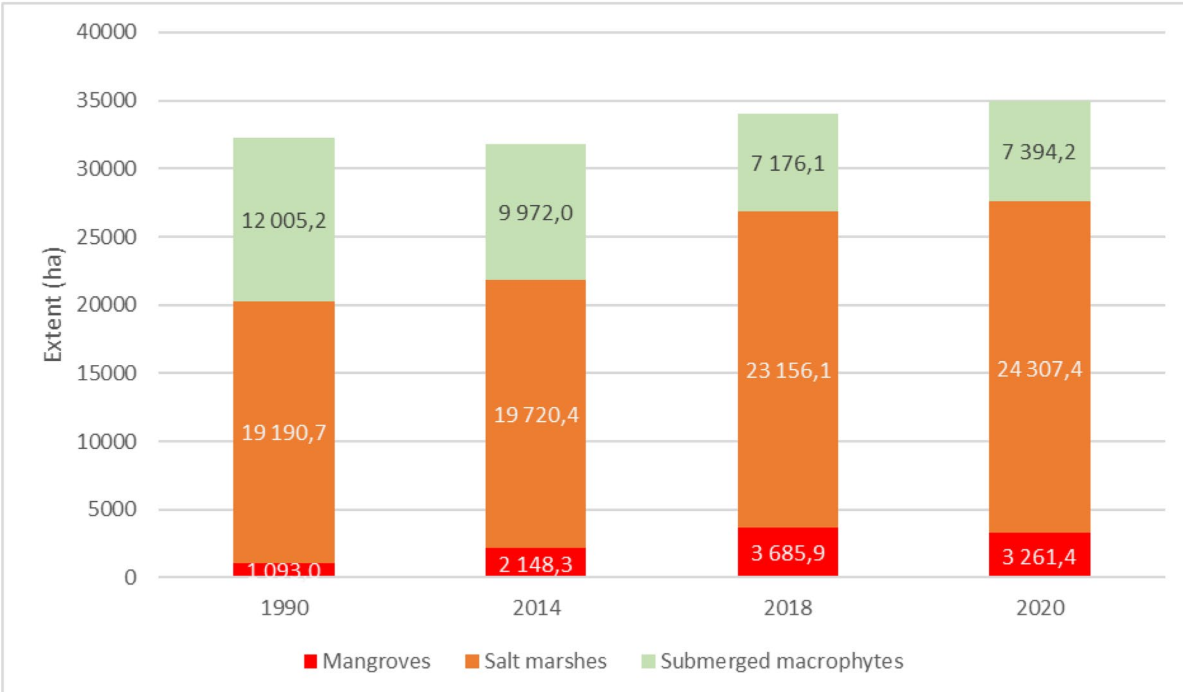

Fig. 3 Changes in the extent of estuarine ecosystem functional groups predicted from Landsat and Sentinel-1 and -2 images between 1990 and 2020 for South Africa

Confidence in the changes in mangrove extent compared to other studies

The outputs of the remote sensing classification extent for mangroves showed an increase across the four time periods from 1990 to 2020, with the 2020 extent reported as 3261.4 ha for a total of 207 (62%) of the total number of 332 South African systems occurring in the Mangrove EO region (Table 1). These estuaries dominate in number but cover less than a third of the extent of the South African coastline, occurring from the Tyolomnqa Estuary in the Eastern Cape Province eastwards to Kosi Estuary at the border with Mozambique. The user's accuracies of mangroves were low for 1990 (66% and 53% for estuarine systems with submerged macrophytes and those without, respectively), while attaining > 81% for 2014, 2018 and 2020. Therefore, only changes between 2014 and 2020 should be considered in reporting, and not those of 1990.

To further explore the confidence of the changes in mangrove extent in South African estuaries, a comparison was made with three other datasets that mapped mangrove extent. The first comparison was between the mangroves resulting from the remote sensing outputs to those manually mapped. The NMU layer mapped mangroves manually with high confidence in extent and presence in only 32 estuaries of South Africa, with historical extent lost in 11 estuaries, and the Tyolomnqa only recently showing emergence of mangroves (Adams et al. 2016, 2019; Raw et al. 2023; Riddin et al. 2024a). The mangrove EO region was, however, mapped more extensively in this paper, from the Nahoon to Kosi, to assess the capabilities of remote sensing to automate monitoring of the mangroves for the subtropical and tropical estuarine bioregions. The mangrove extent resulting from the remote sensing prediction for 2020 (3261.4 ha) resulted in a remote sensing prediction of mangrove extent for 95% (197 of the 207) estuarine systems in the mangrove EO region. This extent makes up 114% of the extent of 2820 ha collated through heads-up digitising in the NMU layer, which mapped habitat cover for only 122 (59%) of the 207 estuaries in the mangrove EO region, of which 32 of the estuaries have confirmed mangrove habitat. Upon individual

Table 4 Percentage of overall and user's accuracies (%) attained from the remote sensing classification reported per class across the four Earth Observation (EO) regions and year

EO region (across)		Not mangroves EO region								Mangrove EO region							
Year (across)		1990		2014		2018		2020		1990		2014		2018		2020	
Class (down) accuracies (across)	Class#	noSM	SM	noSM	SM	noSM	SM	noSM	SM	noSM	SM	noSM	SM	noSM	SM	noSM	SM
Overall accuracies (%, across)		**72.6**	**57.5**	**74.5**	**61.3**	**78.8**	**67.1**	**78.4**	**68.0**	**63.4**	**64.2**	**73.6**	**71.2**	**78.6**	**76.1**	**82.5**	**78.7**
Bare soil	1	0.0	0.0	0.0	0.0	0.0	0.0	100.0	0.0	0	0.0	0.0	0.0	0.0	0.0	0.0	0.0
Beach sand	2	64.3	20.0	100.0	100.0	84.6	100.0	50.0	100.0	61.9	0.0	65.2	66.7	81.8	0.0	75.0	100.0
Built-up areas	3	85.2	69.2	79.2	61.9	85.2	60.0	90.0	56.3	0.0	0.0	0.0	94.1	0.0	95.8	0.0	100.0
Cleared land	4	0.0	50.0	0.0	0.0	0.0	50.0	0.0	0.0	0.0	0.0	0.0	0.0	0.0	0.0	0.0	0.0
Cropland	5	0.0	45.5	0.0	62.1	0.0	65.6	0.0	42.1	57.1	0.0	62.5	0.0	75.0	0.0	66.0	0.0
Cultivated wetland	6	0.0	0.0	0.0	0.0	0.0	0.0	0.0	0.0	0.0	0.0	0.0	65.9	0.0	69.3	0.0	87.7
Forested wetland	7	0.0	0.0	0.0	0.0	0.0	0.0	0.0	0.0	30.0	70.5	55.6	60.8	62.5	72.4	78.6	77.2
Freshwater marsh	8	0.0	0.0	0.0	0.0	0.0	0.0	0.0	0.0	50.0	60.8	42.9	67.2	25.0	61.2	85.7	70.1
Intertidal salt marsh (Other)	9	33.0	100	0.0	100	0.0	0.0	0.0	50	67.0	0.0	86	0.0	78	0.0	100.0	0.0
Intertidal salt marsh (*Spartina maritima*)	10	0.0	38	0.0	63	0.0	85	0.0	85	0.0	0.0	100	0.0	100	0.0	66.7	0.0
Intertidal salt marsh (Succulent)	11	0.0	54	0.0	39	0.0	75	0.0	63	0.0	0.0	0.0	0.0	0.0	0.0	0.0	0.0
Large macrophytes	12	58.8	71.4	46.5	59.2	66.7	66.0	76.2	85.2	41.7	53.2	43.4	59.2	52.7	64.3	63.3	64.4
Mangroves	13	0.0	0.0	0.0	0.0	0.0	0.0	0.0	0.0	53.1	65.9	81.7	84.9	85.4	80.6	86.5	82.7
Mining	14	100.0	69.2	85.7	82.9	100.0	93.8	100.0	87.8	0.0	0.0	0.0	0.0	0.0	0.0	0.0	0.0
Nymphaea spp.	15	0.0	0.0	0.0	0.0	0.0	0.0	0.0	0.0	0.0	0.0	0.0	100.0	0.0	83.3	0.0	50.0
Open water	16	82.8	65.1	89.9	68.2	89.2	72.9	88.2	81.2	60.4	74.0	74.7	73.1	97.5	81.9	91.3	80.8
Relic gardens	17	0.0	0.0	0.0	0.0	0.0	0.0	0.0	0.0	0.0	45.7	0.0	68.8	0.0	84.0	0.0	88.6
Salt marsh	18	47.4	57.7	66.7	63.3	75.0	55.2	54.2	65.9	39.1	100.0	55.0	100.0	100.0	100.0	84.0	50.0
Sand/mudbanks	19	0.0	60.0	0.0	62.1	0.0	63.6	0.0	70.4	0.0	12.5	0.0	50.0	0.0	77.8	0.0	100.0
Submerged macrophytes (intertidal *Zostera*)	20	0.0	0.0	0.0	0.0	0.0	0.0	0.0	0.0	0.0	85.0	0.0	98.1	0.0	89.6	0.0	90.1
Submerged macrophytes (subtidal *Zostera*)	21	0.0	55.6	0.0	63.4	0.0	67.9	0.0	64.1	0.0	65.1	0.0	74.3	0.0	76.5	0.0	78.0
Supratidal salt marsh (*Juncus kraussii*)	22	0.0	100.0	0.0	75.0	0.0	75.0	0.0	60.0	82.4	62.8	66.7	60.7	78.6	78.7	42.9	70.4
Supratidal salt marsh (Other)	23	53.6	55.8	62.7	62.9	67.6	62.4	67.1	62.1	33.3	100.0	66.7	75.0	27.3	73.3	100.0	71.4
Supratidal salt marsh (Saline grasses)	24	0.0	0.0	0.0	0.0	0.0	0.0	0.0	0.0	0.0	42.9	0.0	100.0	100.0	44.4	0.0	75.0
Terrestrial grasses	25	0.0	28.6	0.0	75.0	0.0	20.0	0.0	50.0	76.9	52.4	78.6	57.7	72.0	73.5	93.8	73.5
Terrestrial shrubs	26	0.0	33.3	0.0	33.3	0.0	59.3	0.0	47.1	0.0	0.0	0.0	0.0	0.0	0.0	0.0	0.0
Terrestrial trees	27	0.0	51.7	0.0	73.0	0.0	75.0	0.0	78.8	70.4	67.9	76.8	76.3	79.3	80.3	82.8	81.8
Terrestrial vegetation	28	78.4	57.1	74.7	40.5	74.0	44.8	77.5	55.6	0.0	88.9	0.0	50.0	0.0	85.7	0.0	57.1
Timber plantations	29	0.0	0.0	0.0	0.0	0.0	0.0	0.0	0.0	60.9	100.0	88.8	81.8	82.1	75.0	96.4	83.3
Waves	30	0.0	0.0	0.0	0.0	100.0	0.0	0.0	0.0	0.0	0.0	100.0	0.0	0.0	0.0	0.0	0.0

EO region has no submerged macrophytes; SM EO region has submerged macrophytes. Where the subtypes of salt marshes could not be identified, the term 'Salt marsh' was used comparison to the 32 estuaries that were mapped by NMU, more than half of the estuaries showed an overprediction of mangrove extent of > 115%, with only ten estuaries within 85–115% of the manually-mapped extent (Adams et al. 2016; 2019), and five estuaries an underestimation of the extent < 85% of the NMU mapped extent. The prediction of mangrove extent in these 175 estuaries as outputs from remote sensing classification when using the medium spatial resolution imagery, would benefit from finer spatial resolution imagery to improve the automation of monitoring and the accuracy of detecting mangrove saplings in the field.

Fine-scale manual mapping of mangroves was done with high confidence for the recent red listing of the ecosystem (Riddin et al. 2024a). This was based on site specific data that exists for all mangrove estuaries in South Africa. The comparison of these data with our study showed that the remote sensing outputs have resulted in spectral confusion between the mangroves and forested wetlands or terrestrial pine forests, with contradictory results. This is because these forests often occur together in mosaics and in some systems as a thin, single line of mangrove trees and would require higher spatial resolution imagery for detection and monitoring.

The predicted extent of mangroves made up 115% of the Global Mangrove Watch extent of 2821 ha in 2020 (Bunting et al. 2022). The Global Mangrove Watch recorded an increase of 77 ha of mangrove from 2566 to 2643 ha between 1996 and 2020 for South Africa (Bunting et al. 2022). Mangroves were incorrectly mapped in this dataset for the Keiskamma Estuary where salt marshes occur. In comparison, Landsat images used for 2014 predicted 26–8% more extent compared to the Sentinel image predictions of 2018 and 2020 and showed that the extent of 1990 (1093 ha) doubled by 2014 (2148 ha), which is unlikely.

In contrast, the calculated extent forms 10% of the extent of mangroves (33,000 ha) that were predicted by Bessinger et al. (2022) using a mosaic of Landsat–8 images between 1 January 2018 and 31 December 2019 for estuaries in the Western Cape, Eastern Cape and KwaZulu-Natal Provinces. No mangroves occur in the temperate Western Cape Province, and therefore these predictions are incorrect.

Natural expansion of mangrove canopy cover has been previously observed between 1937 and 1996 at 0.3 km^2/annum for a few estuaries on the eastern shores of South Africa, however, transformation to subsistence agriculture was reported for parts at a rate of 0.4 km^2/annum (Wessels 1997). Finer-scale studies for these areas mapped from aerial photographs show an increase in the mangrove extent for four of the ten estuaries on this stretch of the coastline between 1930 and 2018 (Adams and Rajkaran 2020). Large increases of 50 ha have been observed in the uMlalazi Estuary, owing to the artificial mouth breaching in the 1930s. Other minimal increases have occurred in the Great Kei, Kwelera, Nahoon and Tyolomnqa estuaries totalling less than 5 ha (Riddin et al. 2024a, b).

In some studies, changes in the extent of mangroves derived from Landsat images produced incorrect trends compared to finer scale studies. The Global Mangrove Loss Drivers application that assessed changes in the extent of mangroves between 2000 and 2016, using Landsat images at a 30 m spatial resolution, showed that 62% of the extent of mangroves in the uMhlathuze and Richards Bay estuaries have decreased through erosion (Goldberg et al. 2020). In comparison, finer-scale analysis, indicated expansion of mangrove extent in the uMhlathuze Estuary by 1000 ha over recent years verified by site visits. Finer-scale images used for mapping changes in the extent of mangroves in 2018 (Machite 2023) also found little change in the extent of the mangrove habitats for 16 Eastern Cape estuaries but reported changes in the density of vegetation due to declining ecological condition and increase in pressures such as livestock browsing and cutting of trees.

Visual investigations of the predicted extent of mangroves for 2020 from the Sentinel images also clearly showed overprediction of extent in some areas, and underrepresentation of small, narrow and fragmented mangrove patches. Despite the good accuracies attained in this study for the predictions of years 2014, 2018 and 2020 for the mangroves, the understanding of representativity errors is critical for informing monitoring and reporting to provincial, national and global targets. In the red listing of ecosystems (Bunting et al. 2022), changes in the extent of ecosystems are required across a 50 year period or since 1750. This study only covered four years across a 30 year time period, with poor understanding of how much of the original extent, with natural increase in canopy cover, can be expected. To address this shortcoming, fine-scale mapping from the 1940s

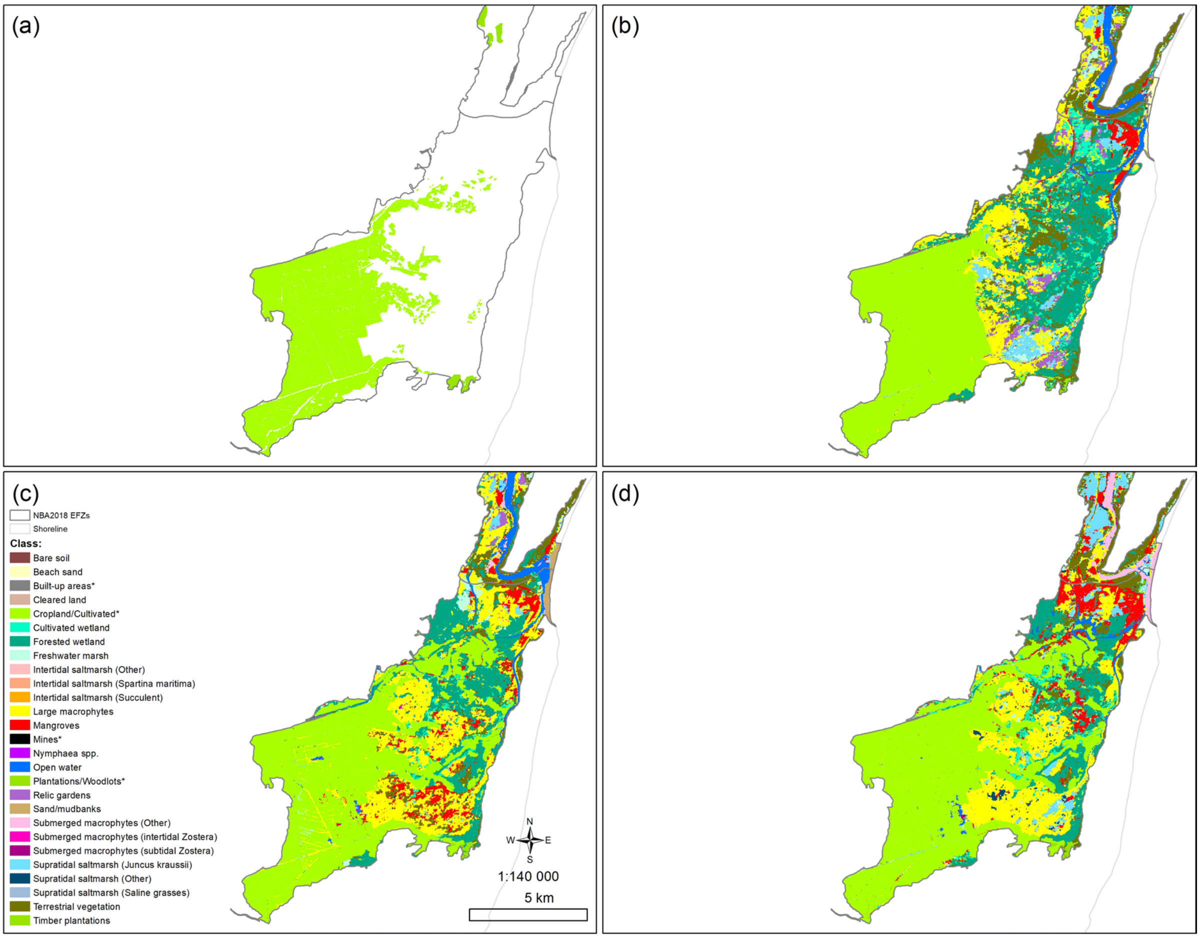

Fig. 4 The distribution of estuarine and freshwater ecosystem functional groups of the iMfolozi/uMsunduze Estuary varies across 4 years: **a** 1990, **b** 2014, **c** 2018 and **d** 2020. Classes with a * indicate those derived from the National Land Cover data

aerial photographs of these estuaries (e.g. Adams and Rajkaran 2020), and more recent fine-scale images would be required to assess the error in representation of change in the layers of our work and those of the Global Mangrove Watch, ranging across more pristine to degraded systems with higher degrees of impacts and pressures.

Confidence in the changes of salt marshes extent compared to other studies

The extent of salt marshes predicted for 2020 from the Sentinel-1 and -2 multi-season images classification (24307 ha) showed an increase of 5116 ha or 127% from the 1990 Landsat image extent. The remote sensing layer predicted coverage across 322 estuaries totalling 165% of the extent reported by NMU for 115 estuaries (14713 ha; Raw et al. 2023). The manually-mapped layer was more than double the extent mapped in the Allen Coral Atlas of 2020 (McOwen et al. 2017). In comparison to the most recent mapping of tidal salt marshes totalling 8973.8 ha (Worthington et al. 2023), the manually-mapped layer showed 16941.8 ha, which is more than double the extent of the global dataset. The global dataset still shows omission and commission errors, even though representing only 53% of the measured extent. This can be attributed to the fact that the manually-mapped layer includes both intertidal and supratidal vegetation; i.e. all salt marsh areas below the 1.5 m above mean sea level contour line. User's accuracies in the mangrove regions were > 78%, whereas those in the

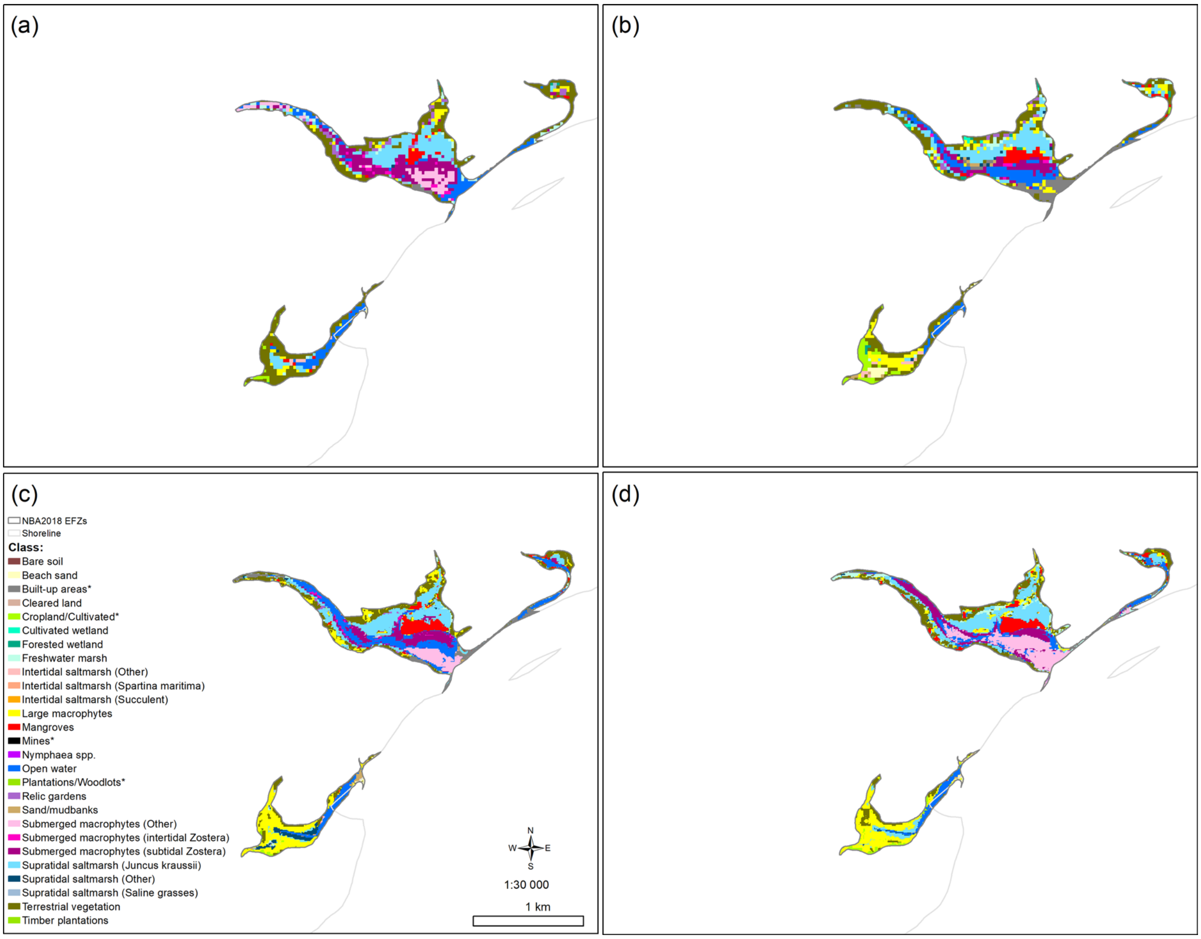

Fig. 5 The distribution of estuarine and freshwater ecosystem functional groups of the Mnyameni Estuary (centre), with the Mtolane Estuary in the south and the micro-estuary 'Subtropical 33' in the north, varies across 4 years: **a** 1990, **b** 2014, **c** 2018 and **d** 2020. Classes with a * indicate those derived from the National Land Cover data

non-mangrove regions varied between 33 and 85% across the four years. Visual image interpretation (Lillesand et al. 2015, p. 59) showed overprediction beyond the 5 m and 10 m above mean sea level contour lines, which are usually used as a guideline for where the estuaries change to freshwater or terrestrial ecosystems (Van Niekerk et al. 2019).

PlanetScope images at approximately 3 m spatial resolution between December 2023 and January 2024 predicted the extent of salt marshes for estuaries between the Orange River (bordering between South Africa and Namibia), and the Coega Estuary in the Eastern Cape Province, as a total of 9130 ha with a user's accuracy of 77% (Campbell et al. xxxx). In comparison, the 2020 prediction of 10 m spatial resolution Sentinel-1 and -2 images, predicted 16677 ha, which is an overestimation of the salt marsh by 183%. In particular, the 'Supratidal saltmarsh (Other)' makes up 85% of the extent of all the salt marshes categories. The capabilities of finer spatial resolution images for mapping and monitoring the salt marshes in general, and their subtypes, remain to be assessed.

Confidence in the changes of submerged macrophyte extent compared to other studies

The extent of submerged macrophytes declined by 4611 ha between 1990 and 2020, totalling 38% of the original extent predicted for 1990. The multi-seasonal

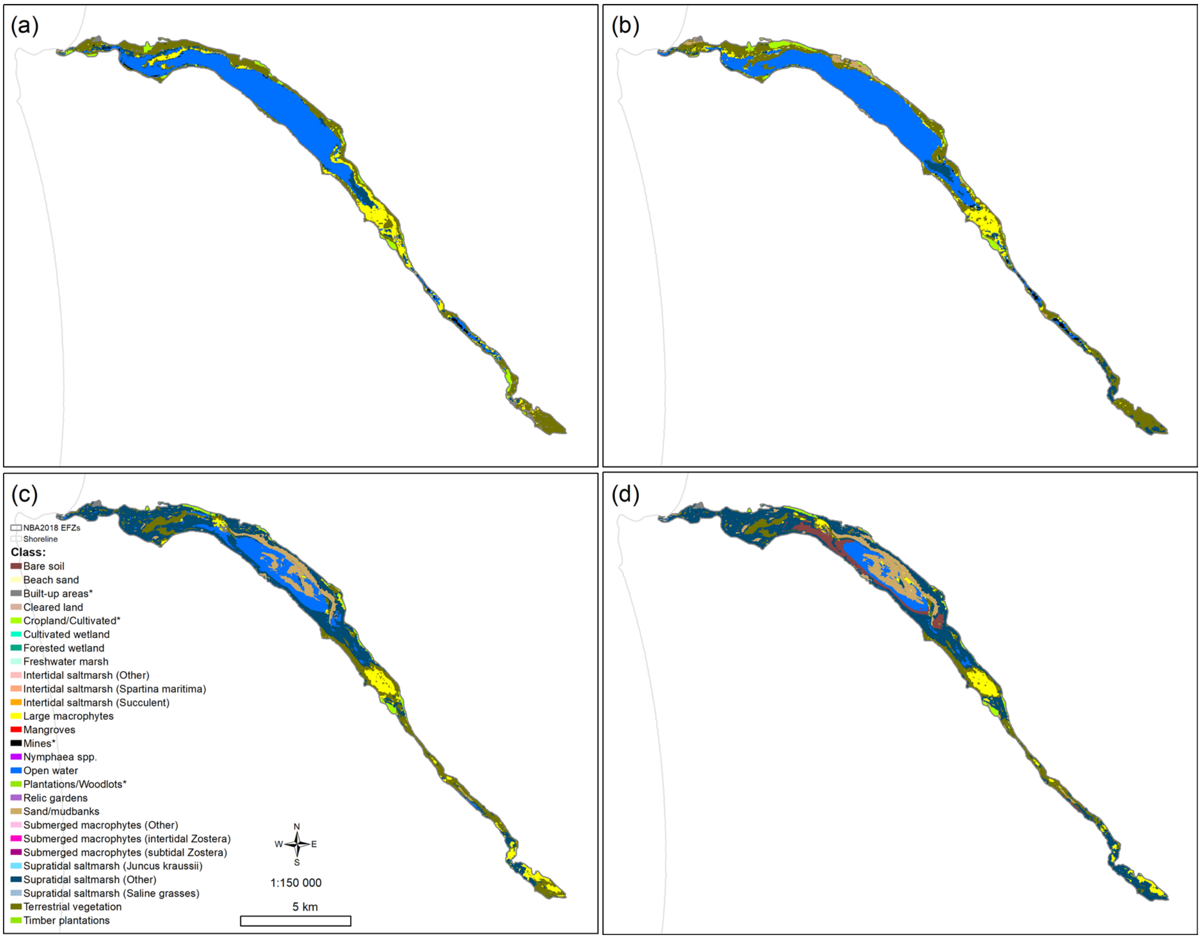

Fig. 6 The distribution of estuarine and freshwater ecosystem functional groups of the Verlorenvlei Estuary varies across 4 years: **a** 1990, **b** 2014, **c** 2018 and **d** 2020. Classes with a * indicate those derived from the National Land Cover data

classification predicted between 410 and 684% of the extent that was mapped for estuaries in the NMU layer (1755 ha; Raw et al. 2023). Only 12% (39 of 332) of the estuaries host submerged macrophytes. In comparison to the global dataset, our remote sensing mapped between 18 to 29% of the extent in Short et al. (2007), which shows a complete overprediction of extent in the global dataset for South African estuaries, compared to the NMU layer. The user's accuracy for submerged macrophytes exceeded 74% for all years in the mangrove EO subregion mapped, except for the subclass Submerged macrophytes (subtidal *Zostera*) that attained 64% user's accuracy in 1990. In the non-mangrove EO region, the user's accuracies for submerged macrophytes were < 68% and insufficient for predicting and monitoring changes in submerged macrophytes.

The classes with *Z. capensis* overpredicted for > 90% of the extent of the open water in the Klein, Langebaan, Swartvlei and Qora estuaries in this study, though showing relatively good extent predictions visually in other systems. Kohlus et al. (2020) compared aerial mapping, ground mapping and Landsat-8 classification for estimation of *Zostera* spp. beds in the Wadden sea. Landsat-8 classification had an 84% accuracy for high density beds (> 60%), compared to 79% accuracy for Sentinel-2 classification. Beds of low density, i.e. those that occurred in small channels, were not always detected correctly when compared to fine scale mapping (Landsat-8 68% and Sentinel-2 86%) with a tendency to underestimate extent, especially in the bed density range of 10–40%. However, aerial mapping and in situ transect mapping both show a more generalised outline. In South Africa, *Zostera capensis* often forms narrow bands along the sides of the estuary channel, or on the water side of mangrove stands (Adams 2016) making classification of them through remote sensing difficult at a spatial resolution of ≥ 10 m.

The extent of submerged macrophytes between the Orange River and Coega estuaries from the PlanetScope images (Campbell et al. xxxx) resulted in 1718 ha with a user's accuracy of 67%. The outputs from the 10 m spatial resolution Sentinel-1 and -2 images in this study predicted the extent of the submerged macrophytes for the same area as 6133 ha, or 357% more, for the year 2020. Finer spatial resolution images should be pursued for mapping and monitoring the subtypes of the submerged macrophytes.

The use of multitemporal images can contribute to distinguishing supratidal from intertidal salt marshes and intertidal from subtidal seagrass areas, across the hydrological complexity and tidal variation of different estuarine ecosystem types. However, using multi-seasonal images from medium spatial resolution sensors in the prediction of submerged macrophytes extent is therefore not advised. These are dynamic ecosystems where die-off and spatial changes occur naturally, in response to natural drivers such as estuary mouth state, ambient water level, turbidity and salinity (Adams 2016). The stacking of multiple images, across various inundation and mouth states, contributed to spectral confusion between water and submerged macrophytes, resulting in overestimations of extent. In the visual comparison of the results with multiple images, this study measured the extent of the submerged macrophytes occurrence in Google Earth Pro images relative to centre points of some of the Sentinel-2 pixels and found it hard to secure dense areas with > 70% cover to use as sample points in the classification. The extent of these submerged macrophytes also showed variation across mouth states and estuarine types. Classifications of salt marshes with individual time-stamp Sentinel-2 images for three estuaries in the Western Cape attained user's accuracies > 70 (Struwig 2022). This means that mapping of submerged macrophytes may require specific time-definite images for classification (not stacked), and understanding the changes relative to the mouth states, and how these should be considered for national and global reporting to targets.

Conclusions

The outputs of our assessment showed changes in the extent of mangroves, salt marshes and submerged macrophytes for 4 years (1990, 2014, 2018 and 2020) for 332 South African estuaries. We have a medium confidence that the multi-season Sentinel image classifications were able to map the extent of mangroves and can potentially be used for monitoring changes in these ecosystems over time. However, further work is required to quantify the representativity errors and the degree to which degradation can be detected and monitored.

In contrast, the use of multi-season images in the classification of salt marshes and submerged macrophytes results in extensive overprediction across all years. Improvements should be investigated in the ability of time-series analysis to quantify changing extents in relation to estuary mouth states and hydrological cycles and distinguish natural changes from those resulting from anthropogenic and/or climate change.

Quantifying changes in estuaries are important for GBF reporting and early intervention, as is demonstrated by the case of the Verlorenvlei Estuary (Fig. 6), a Ramsar site, that is now recommended for the Montreux list (Riddin et al. 2024b). Comparisons with historic and current finer scale, and finer spatial resolution images are critical to determine the representativity errors of extent of the coarse-scale Landsat and Sentinel images, and their sensitivity in detecting changes over time, for the three main estuarine EFGs, and their subtypes.

Acknowledgements Zane Silinda from GIZ is sincerely thanked for his project management. Members of the project organising committee are thanked for input on the research findings; Zane Silinda, Anna Klaverkamp, Mathias Bertram, Juliette Noppe (from GIZ) and Barney Kgope, Hlengiwe Mbatha, Itchell Guiney, Khodani Mavhungu, Lungile Moyo and Mbulelo Dopolo (from Department of Forestry, Fisheries and Environment, South Africa). The National Research Foundation of South Africa through the support of the DSI/NRF Research Chair in Shallow Water Ecosystems supported JBA and is thanked for funding (UID 84375).

Author contributions Conceptualisation, L.v.N.; H.v.D.; J.A.; methodology, H.v.D.; P.A.; T.R.; sample generation, H.v.D.; P.A.; T.R.; A.M.; E.W.; A.M; validation, H.v.D.; P.A.; T.R.; A.M.; E.W.; A.M; formal analysis, H.v.D. and P.A.; writing—original draft preparation, H.v.D.; writing—review and editing, H.v.D.; P.A.; T.R.; A.M.; E.W.; A.M.; L.v.N.; J.A.; All authors have read and agreed to the published version of the manuscript.

Funding Open access funding provided by Council for Scientific and Industrial Research. This research was funded by the Deutsche Gesellschaft für Internationale Zusammenarbeit (GIZ) GmbH, through the implemented Climate Support Programme, as part of the International Climate Initiative (IKI). The German Federal Ministry for the Environment, Nature Conservation, Nuclear Safety and Consumer Protection (BMUV) supports the IKI on the basis of a decision adopted by the German Bundestag.

Data availability Available on request.

Declarations

Competing interests The authors declare no competing interests.

References

Adams JB (2016) Distribution and status of *Zostera capensis* in South African estuaries—a review. S Afr J Bot 107:63–73. https://doi.org/10.1016/j.sajb.2016.07.007

Adams JB, Rajkaran A (2020) Changes in the mangroves at their southernmost African distribution limit. Estuar Coast Shelf Sci 247:106862. https://doi.org/10.1016/j.ecss.2020.106862

Adams JB, Veldkornet D, Tabot P (2016) Distribution of macrophyte species and habitats in South African estuaries. S Afr J Bot 107:5–11. https://doi.org/10.1016/j.sajb.2016.08.001

Adams JB, Fernandes M., Riddin T (2019) Chapter 5: Estuarine habitat extent and trend. In: Van Niekerk L, Adams JB, Lamberth SJ, MacKay F, Taljaard S, Turpie JK, Weerts S, Raimondo DC (eds.) South African National Biodiversity Assessment 2018: Technical Report. Volume 3: Estuarine Realm. Council for Scientific & Industrial Research (CSIR) report number CSIR/SPLA/EM/EXP/2019/0062/A. South African National Biodiversity Institute (SANBI), Pretoria, South Africa. Report Number: SANBI/NAT/NBA2018/2019/Vol3/A. pp 52–75

Allen Coral Atlas (2020) Imagery, maps and monitoring of the world's tropical coral reefs. https://zenodo.org/records/6622015. Accessed 14 Dec 2021

Apleni P, Van Deventer H, Naidoo L, Tsele P (In prep). Quantifying the extent and rate of changes in wetland types of the Maputaland Coastal Plain with remote sensing.

Bessinger M, Lück-Vogel M, Skowno A, Conrad F (2022) Landsat-8 based coastal ecosystem mapping in South Africa using Random Forest classification in Google Earth Engine. S Afr J Bot 150:928–929. https://doi.org/10.1016/j.sajb.2022.08.014

Breiman L (2001) Random forests. Mach Learn 45:5–32

Bunting P, Rosenqvist A, Hilarides L, Lucas RM, Thomas N, Tadono T, Worthington TA, Spalding M, Murray NJ, Rebelo LM (2022) Global mangrove extent change 1996–2020: global mangrove watch version 3.0. Remote Sens 14:3657

Campbell AD, Adam E, Adams JB, Barrenblit A, Fatoyinbo L, Fisher R, Jensen D, Naidoo L, Ridden T, Simard M, Smith K, Thakali P, Van Deventer H, Van Niekerk L, Stovall A (In prep) Monitoring coastal estuarine habitats for biodiversity along the temperate bioregion of South Africa.

Convention on Biological Diversity (CBD) (2022) Nations adopt four goals, 23 targets for 2020 in landmark UN biodiversity agreement. CBD, Montreal, Canada. https://www.cbd.int/article/cop15-cbd-press-release-final-19dec2022. Accessed 9 Mar 2024

Environmental Systems Research Institute (ESRI) (1999–2018) ArcGIS desktop 10.7, Redlands, CA, ESRI, United States of America. https://www.esri.com/en-us/home

Gao BC (1996) NDWI—a normalized difference water index for remote sensing of vegetation liquid water from space. Remote Sens Environ 58:257–266. https://doi.org/10.1016/S0034-4257(96)00067-3

GeoTerraImage (GTI) Pty Ltd (2015a) 1990 South African National Land-Cover Dataset. DEA/CARDNO SCPF002: Implementation of land-use maps for South Africa. Project Specific Data User Report and Metadata version 05. South African Department of Environment Forestry and Fisheries (DFFE), Pretoria, South Africa. http://egis.environment.gov.za

GeoTerraImage (GTI) Pty Ltd (2015b) The 2013–2014 South African National Land-Cover Dataset, 2013–14 SA Landcover report. Contents version 05 (DEA open access). Data User Report and Metadata. South African Department of Environment Forestry and Fisheries (DFFE), Pretoria, South Africa. http://egis.environment.gov.za

GeoTerraImage (GTI) Pty Ltd (2019) 2018 South African national land cover dataset version 4. South African Department of Environment Forestry and Fisheries (DFFE), Pretoria, South Africa. http://egis.environment.gov.za

GeoTerraImage (GTI) Pty Ltd (2021) 2020 South African national land cover dataset. South African Department

of Environment Forestry and Fisheries (DFFE), Pretoria, South Africa. http://egis.environment.gov.za
Google Earth Pro (GEP) Version 7.3.3.7786 (1985–2022) Various images composites available in GEP for the Estuarine Functional Zones of South Africa. Available from the server kh.google.com and http://www.earth.google.com
Giri C, Ochieng E, Tieszen LL, Zhu Z, Singh A, Loveland T, Masek J, Duke N (2011) Status and distribution of mangrove forests of the world using earth observation satellite data (version 1.3, updated by UNEP-WCMC). Glob Ecol Biogeogr 20:154–159. https://doi.org/10.1111/j.1466-8238.2010.00584.x
Gitelson A, Merzlyak MN (1994) Spectral reflectance changes associated with autumn senescence of *Aesculus hippocastanum* L. and *Acer platanoides* L. leaves spectral features and relation to chlorophyll estimation. J Plant Physiol 143(3):286–292. https://doi.org/10.1016/S0176-1617(11)81633-0
Gitelson AA, Kaufman YJ, Merzlyak MN (1996) Use of a green channel in remote sensing of global vegetation from EOS-MODIS. Remote Sens Environ 58(3):289–298. https://doi.org/10.1016/S0034-4257(96)00072-7
Goldberg L, Lagomasino D, Thomas N, Fatoyinbo T (2020) Global declines in human-driven mangrove loss. Glob Change Biol 26:5844–5855. https://doi.org/10.1111/gcb.15275
Gorelick N, Hancher M, Dixon M, Ilyushchenko S, Thau D, Moore R (2017) Google earth engine: planetary-scale geospatial analysis for everyone. Remote Sens Environ 202(1):18–27. https://doi.org/10.1016/j.rse.2017.06.031
Green EP, Short FT (2003) World Atlas of Seagrasses. Prepared by UNEP World Conservation Monitoring Centre. Berkeley (California, USA): University of California, United States of America, pp 332. https://archive.org/details/worldatlasofseag03gree
Greifeneder F, Notarnicola C, Hahn S, Vreugdenhil M, Reimer C, Santi E, Paloscia S, Wagner W (2018) The added value of the VH/VV polarization-ratio for global soil moisture estimations from scatterometer data. IEEE J Sel Top Appl Earth Obs. https://doi.org/10.1109/jstars.2018.2865185
Harris LR, Bessinger M, Dayaram A, Holness S, Kirkman S, Livingstone TC, Lombard AT, Lück-Vogel M, Pfaff M, Sink KJ, Skowno AL, Van Niekerk L (2019) Advancing land-sea integration for ecologically meaningful coastal conservation and management. Biol Conserv 237:81–89. https://doi.org/10.1016/j.biocon.2019.06.020
Huete A, Didan K, Miura T, Rodriguez EP, Gao X, Ferreira LG (2002) Overview of the radiometric and biophysical performance of the MODIS vegetation indices. Remote Sens Environ 83(1–2):195–213. https://doi.org/10.1016/S0034-4257(02)00096-2
Keith DA, Ferrer-Paris JR, Nicholson E, Bishop MJ, Polidoro BA, Ramirez-Llodra E, Tozer MG, Nel JL, MacNally R, Gregr EJ, Watermeyer KE, Essl F, Faber-Langendoen D, Franklin J, Lehmann CER, Etter A, Roux DJ, Stark JS, Rowland JA, Brummitt NA, Fernandez-Arcaya UC, Suthers IM, Wiser SK, Donohue I, Jackson LJ, Pennington RT, Iliffe TM, Gerovasileiou V, Giller P, Robson BJ, Pettorelli N, Andrade A, Lindgaard A, Tahvanainen T, Terauds A, Chadwick MA, Murray NJ, Moat J, Pliscoff P, Zager I, Kingsford RT (2022) A function-based typology for Earth's ecosystems. Nature 610:513–518. https://doi.org/10.1038/s41586-022-05318-4
Kohlus J, Stelzer K, Müller G, Smollich S (2020) Mapping seagrass (*Zostera*) by remote sensing in the Schleswig-Holstein Wadden Sea. Estuar Coast Shelf Sci 238:106699. https://doi.org/10.1016/j.ecss.2020.106699
Lillesand T, Kiefer RW, Chipman J (2015) Remote sensing and image interpretation, 7th Ed. p 736
Machite A (2023) Changes in mangroves along the Eastern Cape coast of South Africa. MSc dissertation at the Faculty of Science, Nelson Mandela University, Gqeberha, South Africa
Mahdianpari M, Jafarzadeh H, Granger JE, Mhamadimanesh F, Brisco B, Salehi B, Homayouni S, Weng W (2020) A large-scale change monitoring of wetlands using time series Landsat imagery on Google Earth Engine: a case study in Newfoundland. Gisci Remote Sens 57(8):1102–1124. https://doi.org/10.1080/15481603.2020.1846948
Mcowen C, Weatherdon LV, Bochove J, Sullivan E, Blyth S, Zockler C, Stanwell-Smith D, Kingston N, Martin CS, Spalding M, Fletcher S (2017) A global map of saltmarshes (ver 6.0). Biodivers Data J 5:e11764. https://doi.org/10.3897/BDJ.5.e11764
Qi J, Chehbouni A, Huete AR, Kerr YH, Sorooshian S (1994) A modified soil adjusted vegetation index. Remote Sens Environ 48(2):119–126. https://doi.org/10.1016/0034-4257(94)90134-1
Raw JL, Van Niekerk L, Chauke O, Mbatha H, Riddin T, Adams JB (2023) Blue carbon sinks in South Africa and the need for restoration to enhance carbon sequestration. Sci Total Environ 859:160142. https://doi.org/10.1016/j.scitotenv.2022.160142
Reuter R (2011) SEOS—Earsel's project on science education through earth observation for high schools. Int Arch Photogramm Remote Sens Spatial Inf Sci 2011:7–10
Riddin T, Van Niekerk L, Strange F, Adams JB (2024b) Habitat changes in response to pressures in the Verlorenvlei Estuarine Lake, South Africa. S Afr J Sci. https://doi.org/10.17159/sajs.2024/16868
Riddin T, Adams JB, Rajkaran A, Machite A, Peer N, Suárez EL (2024a) IUCN red list of ecosystems, Mangroves of the Agulhas. https://doi.org/10.32942/X2H322
Rondeaux G, Steven M, Baret F (1996) Optimization of soil-adjusted vegetation indices. Remote Sens Environ 55(2):95–107. https://doi.org/10.1016/0034-4257(95)00186-7
Rouse J, Hass R, Schell J, Deering D (1973) Monitoring vegetation systems in the great plains with ERTS. Third ERTS Symposium, NASA, SP–351 I, 309–317. https://ntrs.nasa.gov/archive/nasa/casi.ntrs.nasa.gov/19740022614.pdf
Satellite Imaging Corporation (2005) Introduction to remote sensing: 3. Resolution. https://seos-project.eu/remotesensing/remotesensing-c03-p02.html
Satellite Imaging Corporation (no date a) Satellite remote sensing systems: characterization of satellite remote sensing systems. https://www.satimagingcorp.com/services/resources/characterization-of-satellite-remote-sensing-systems/

Satellites in Global Development (no date b) Spatial Resolution. https://landscape.satsummit.io/capture/resolution-considerations.html

Science Education through Earth Observation for High Schools (SEOS) (2024) Introduction to remote sensing: 3. Resolution. https://seos-project.eu/remotesensing/remotesensing-c03-p02.html

Short G, Carruthers T, Dennison W, Waycott M (2007) Global seagrass distribution and diversity: a bioregional model. J Exp Mar Biol 350:3–20. https://doi.org/10.1016/j.jembe.2007.06.012

Snyder JP (1993) Flattening the earth: two thousand years of map projections. University of Chicago Press, United States of America. https://doi.org/10.2307/3059630

Snyder JP (1987) Map projections—a working manual. United States Geological Survey Professional Paper 1395. United States Government Printing Office, Washington, United States of America. https://doi.org/10.3133/pp1395

Spalding MD, Kainuma M, Collins L (2010) World Atlas of Mangroves (version 3.1). A collaborative project of ITTO, ISME, FAO, UNEP-WCMC, UNESCO-MAB, UNU-INWEH and TNC. London (UK): Earthscan, London, pp 319. https://doi.org/10.34892/w2ew-m835

Sripada R (2005) Determining in-season nitrogen requirements for corn using aerial color-infrared photography. Ph.D. dissertation, North Carolina State University. https://repository.lib.ncsu.edu/handle/1840.16/4200

Story M, Congalton R (1986) Accuracy assessment: a user's perspective. ISPRS J Photogramm Remote Sens 52:397–399

Struwig J (2022) Determining the duration of open and closed estuarine mouth states and associated habitat types for improved environmental management of estuaries in the Western Cape. Honours dissertation at the Department of Geography, Geoinformatics and Meteorology, University of Pretoria (UP). UP, Pretoria, South Africa

Tessler ZD, Vörösmarty CJ, Grossberg M, Gladkova I, Aizenman H, Syvitski JPM, Foufoula-Georgiou I (2015) Profiling risk and sustainability in coastal deltas of the world. Science 349(6248):638–643. https://doi.org/10.1126/science.aab3574

Tucker CJ (1979) Red and photographic infrared linear combinations for monitoring vegetation. Remote Sens Environ 8(2):127–150. https://doi.org/10.1016/0034-4257(79)90013-0

Ustin SL, Middleton EM (2021) Current and near-term advances in Earth observation for ecological applications. Ecol Process. https://doi.org/10.1186/s13717-020-00255-4

Van Deventer H, Cho MA, Mutanga O (2017) Improving the classification of six evergreen subtropical tree species with multi-season data from leaf spectra simulated to WorldView-2 and RapidEye. Int J Remote Sens 38:4804–4830. https://doi.org/10.1080/01431161.2017.1320445

Van Deventer H, Van Niekerk L, Adams J, Dinala MK, Gangat R, Lamberth SJ, Lötter M, Mbona N, MacKay F, Nel JL, Ramjukadh CL, Skowno A, Weerts SP (2020) National Wetland Map 5—an improved spatial extent and representation of inland aquatic and estuarine ecosystems in South Africa. Water SA 46:66–79. https://doi.org/10.17159/wsa/2020.v46.i1.7887

Van Deventer H, Adams J, Durand JF, Grobler R, Grundling PL, Janse van Rensburg S, Jewitt D, Kelbe B, MacKay CF, Naidoo L, Nel JL, Pretorius L, Riddin T, Van Niekerk L (2021) Conservation conundrum—red listing of subtropical-temperate coastal forested wetlands of South Africa. Ecol Indic 130:108077. https://doi.org/10.1016/j.ecolind.2021.108077

Van Deventer H, Linström A, Naidoo L, Job N, Sieben EJJ, Cho MA (2022) Comparison between Sentinel–2 and WorldView–3 sensors in mapping wetland vegetation communities of the Grassland Biome of South Africa, for monitoring under climate change. Remote Sens Appl Soc Environ. https://doi.org/10.1016/j.rsase.2022.100875

Van Niekerk L, Adams JB, Lamberth SJ, MacKay CF, Taljaard S, Turpie JK, Weerts SP, Raimondo DC (2019) South African National biodiversity assessment 2018: Technical Report. Volume 3: Estuarine Realm. South African National Biodiversity Institute, Pretoria, South Africa. https://doi.org/10.2989/16085914.2019.1685934

Weitkamp T, Karimi P (2023) Evaluating the effect of training data size and composition on the accuracy of smallholder irrigated agriculture mapping in Mozambique using remote sensing and machine learning algorithms. Remote Sens 15(12):3017. https://doi.org/10.3390/rs15123017

Wessels NG (1997) Aspects of the ecology and conservation of swamp forests in South Africa. Unpublished M. Tech thesis, Port Elizabeth Technikon, Port Elizabeth, South Africa, p 155

Worthington TA, Zu Ermgassen PSE, Friess DA, Krauss KW, Lovelock CE, Thorley J, Tingey R, Woodroffe CD, Bunting P, Cormier N, Lagomasino D, Lucas R, Murray NJ, Sutherland WJ, Spalding M (2020) A global biophysical typology of mangroves and its relevance for ecosystem structure and deforestation. Sci Rep 10:14652. https://doi.org/10.1038/s41598-020-71194-5

Worthington TA, Spalding M, Landis E, Maxwell TL, Navarro A, Smart LS, Murray NJ (2023) The distribution of global tidal marshes from earth observation data. https://doi.org/10.1101/2023.05.26.542433

Xu H (2006) Modification of normalised difference water index (NDWI) to enhance open water features in remotely sensed imagery. Int J Remote Sens 27(14):3025–3033. https://doi.org/10.1080/01431160600589179